On Robustness of the Explanatory Power of Machine Learning Models

Banamali Panigrahi[1], Saman Razavi[2,3,4,*], Lorne E. Doig[1], Blanchard Cordell[4], Hoshin V Gupta[5], and Karsten Liber[1,2]

[1]Toxicology Centre, University of Saskatchewan, Canada.

[2]School of Environment and Sustainability, University of Saskatchewan, Saskatoon, Canada.

[3]Institute for Water Futures, Mathematical Sciences Institute, Australian National University, Canberra, Australia.

[4]Global Institute for Water Security, School of Environmental and Sustainability, University of Saskatchewan, Saskatoon, Canada.

[5]Department of Hydrology and Atmospheric Sciences, The University of Arizona, Tucson, Arizona, USA.

[*]Address correspondence to saman.razavi@usask.ca

Abstract:

Machine learning (ML) is increasingly considered the solution to environmental problems where only limited or no physico-chemical process understanding is available. But when there is a need to provide support for high-stake decisions, where the ability to *explain* possible solutions is key to their acceptability and legitimacy, ML can come short. Here, we develop a method, rooted in formal *sensitivity analysis* (SA), that can detect the primary controls on the outputs of ML models. Unlike many common methods for *explainable artificial intelligence* (XAI), this method can account for complex multi-variate distributional properties of the input-output data, commonly observed with environmental systems. We apply this approach to a suite of ML models that are developed to predict various water quality variables in a pilot-scale experimental pit lake.

A critical finding is that subtle alterations in the design of an ML model (such as variations in random seed for initialization, functional class, hyperparameters, or data splitting) can lead to entirely different representational interpretations of the dependence of the outputs on explanatory inputs. Further, models based on different ML families (decision trees, connectionists, or kernels) seem to focus on different aspects of the information provided by data, although displaying similar levels of predictive power. Overall, this underscores the importance of employing ensembles of ML models when explanatory power is sought. Not doing so may compromise the ability of the analysis to deliver robust and reliable predictions, especially when generalizing to conditions beyond the training data.

Key Points:

- We extend the sensitivity analysis (SA) paradigm to handle complex multivariate distributions encountered in machine learning (ML).
- We apply our new SA-based method to explain the controls of various ML models developed for water quality predictions.
- We show different how ML models may rely on entirely different predictors and data signals despite exhibiting comparable predictive power.

1. Introduction

Machine learning (ML) is increasingly used in various domains, and success stories abound for problems that do not carry significant risks of negative consequences. However, when erroneous predictions can have major adverse implications for societal and environmental well-being, ML often faces acceptability and legitimacy challenges *(Lipton, 2017; Lakkaraju et al., 2019; Read et al., 2019; Rudin, 2019; Samek et*

al., 2019; Coyle and Weller, 2020; Lakkaraju et al., 2020; Roscher et al., 2020; Slack et al., 2021; Slack et al., 2023). In such cases, a prime concern is often the difficulty in explaining the reasoning behind an ML model's predictions, which often leads decision makers to favor process-based models (PBMs) that rely on representations that encode a physico-chemical understanding of the underlying system (*Hipsey et al., 2015; Fatichi et al., 2016; Read et al., 2019; Razavi, 2021; Razavi et al., 2022*). However, for many emerging, site-specific environmental problems, such PBMs are not yet readily available.

In recent years, there has been a growing emphasis on the need for *explainable artificial intelligence* (XAI) methods. Various approaches to this have been developed, including *Partial Dependence Plots* (PDP; *Friedman, 1991*), *Permutation Feature Importance* (PFI; *Strobl et al., 2008*), *Local Interpretable Model-agnostic Explanations* (LIME; *Ribeiro et al., 2016*), and *SHapley Additive exPlanations* (SHAP; *Lundberg and Lee, 2017*). These methods are designed to elucidate the specific contributions by which individual feature instances lead to particular outputs (i.e., local interpretation), or to uncover how features collectively influence model outputs across all instances (i.e., global interpretation).

While significant strides have recently been made in XAI, they continue to suffer from limitations. For instance, the widely-used SHAP technique, which is based on game theory, is (1) limited in its scalability to large, high-dimensional datasets due to computational constraints (*Molnar, 2020; Molnar, 2022; Stein et al., 2022*), (2) unable to capture interactions (especially higher-order ones) between features, which may limit its ability to provide comprehensive explanations (*Kumar et al., 2020; Puy et al., 2022*), and further may (3) assign excessive importance to improbable instances, potentially leading to unreliable outcomes (*Molnar, 2022; Rudin et al., 2022*). Various strategies to tackle these limitations have had varying degrees of success (*Owen, 2014; Strumbelj and Kononenko, 2014; Mase et al., 2019; Do and Razavi et al., 2020; Frye et al., 2020; Janzing et al., 2020; Lundberg et al., 2020; Sheikholeslami et al., 2021; Aas et al., 2021; Liu et al., 2024*).

More recently, *sensitivity analysis* (SA) has emerged as an alternative approach to XAI (*Razavi et al., 2021; Scholbeck et al., 2023*). SA is a relatively young discipline that aims to study how the outputs of a model are related to, and are influenced by, its inputs and/or controlling factors (*Saltelli et al., 2021*). The application of SA to ML models has gained traction in recent years, as evidenced by studies such as those by *Tunkiel et al. (2020), Paleari et al. (2021), Fel et al. (2021), Kuhnt and Kalka (2022), Ojha et al. (2022),* and *Stein et al. (2022)*. Unlike conventional XAI methods like SHAP, which focus primarily on individual data instances to evaluate feature importance, SA takes a broader approach by seeking to characterize the entire '*response surface'* of a model – the hyperplane that maps the input variables onto the output of interest. Consequently, the computational demand of SA can be independent of the dataset size used for model training/calibration.

Various SA methods have been developed across different application disciplines. Broadly categorized in *Razavi et al. (2021)*, these methods fall under four main approaches*: derivative-based* (*Morris, 1991; Campolongo et al., 2007; Sobol' and Kucherenko, 2009; Lamboni et al., 2013; Rakovec et al., 2014; Kucherenko and Iooss, 2016; Kucherenko and Song, 2016*), *distribution-based* (*Sobol', 1993; Owen, 1994; Homma and Saltelli, 1996; Saltelli et al., 2008; Kucherenko and Song, 2016; Puy et al., 2021*), *variogram-based* (*Razavi and Gupta, 2016b; Sheikholeslami and Razavi, 2020; Becker, 2020; Alipour et al., 2022*), and *regression-based* (*Kleijnen, 1995; Kambhatla and Leen, 1997; Tonkin and Doherty, 2005; Shin et al., 2013*). These approaches offer different definitions of sensitivity, vary in computational demand, and exhibit varying degrees of scalability to the input space dimension (*Razavi and Gupta, 2015*). While methods under any of these approaches can, in theory, be applied to characterize the importance of inputs in an ML model, a significant challenge arises when dealing with correlated inputs following complex multi-variable distributions. This issue is prevalent across the majority, if not all, SA methods and poses a considerable hurdle in using SA for explainable ML.

Here, we introduce an SA-based method specifically tailored for XAI. We accomplish this by extending the *Variogram Analysis of Response Surface* (VARS) framework (*Razavi and Gupta, 2016b*) to accommodate input-output datasets characterized by complex, multi-variable distributions commonly encountered in ML applications. VARS is a variogram-based method known for its high computational efficiency, even in high-dimensional problems (*Becker, 2020*). It stands out as the only method that considers crucial information regarding the structure of the response surface and perturbation scale (*Haghnegahdar and Razavi, 2017*). Consequently, our new SA method is well equipped to address the three challenges commonly encountered in XAI, as outlined above. It achieves this by being independent of the available data size, adept at handling correlated inputs with any complex marginal distributions, and capable of directly operating on the response surface, thereby ensuring robustness against improbable areas of input space.

We test this approach across a suite of ML models based on decision trees, connectionism, and kernels, as a possible solution to investigate the processes in a pilot pit lake in the Athabasca Oil Sands region of Western Canada. This pilot lake contains fluid tailings treated using the permanent aquatic storage structure process, capped with a blend of oil sands process-affected water and runoff water from the surrounding landscape. We show how the new SA approach illuminates the key controls of different ML models in this environmental system. We show, in particular, that while different ML models may demonstrate similar predictive power, they may do so based on fundamentally different signals and patterns extracted from the data. We also show that ML models based on the connectionism paradigm (including deep learning) may not necessarily be robust to randomness in their initialization, so that multiple replicates of the same model trained to the same data might utilize different underlying relationships to predict the output. We discuss how the understanding of hidden differences across different ML models is critical to enabling learning about physico-chemical processes in the systems under investigation, and to ensure that any decision made on this basis is supported by well-justified explanations.

2. The Sensitivity Analysis (SA) Method

We introduce a general approach, grounded in sensitivity analysis (SA), to illuminating the workings of any model, even a black box, by assessing the extent to which different inputs influence its outputs. This SA-based approach is especially applicable to the problem of "*explainability*" in artificial intelligence (AI), because it addresses three common challenges encountered in machine learning (ML) applications, as detailed in Section 1. In the rest of this section, we present an overview of the underlying VARS-based framework, highlighting its computational efficiency even for models with high-dimensional input spaces. Subsequently, we demonstrate how we extend this framework to handle models with correlated inputs characterized by complex marginal distributions.

2.1. Variogram Analysis of Response Surfaces (VARS)

The VARS framework, originally developed by *Razavi and Gupta (2016a and b)*, aims to characterize the entire '*response surface*' of a model by integrating the directional variograms of a model output over the entire input space and across the full range of '*perturbation scales*', h, as follows:

$$\gamma(h) = \frac{1}{2} V[Z(\boldsymbol{\theta} + h) - Z(\boldsymbol{\theta})] \quad (1)$$

$$\Gamma(H) = \frac{1}{2} \int_0^H V[Z(\boldsymbol{\theta} + h) - Z(\boldsymbol{\theta})] dh \quad (2)$$

where $\gamma(.)$ and $\Gamma(.)$ are directional variogram and integrated variogram functions, respectively, $\boldsymbol{\theta} = \{\theta_i \text{ for } i = 1, \dots, n\}$ and Z represent a point in the input space and its respective model output, n is the total number of inputs, V[ ] denotes the variance operator, and H is the range of perturbation scales of interest.

Figure 1 provides an illustrative graphical representation of directional variograms and their integrated versions. Directional variograms characterize the variance of change in the response surface ($Z(\theta + h) - Z(\theta)$) as a function of perturbation scale (h). For small values of h, this variance of change resembles information akin to derivative-based SA for different inputs, while for larger values, variograms offer insights into the variance contribution of each input, akin to variance-based SA. Thus, VARS serves as a unifying theory bridging derivative-based and variance-based SA, while offering a spectrum of information on the response surface structure for all other values of h. When H is 50 percent of the input range, the respective integrated variogram (IVARS-50) is called the '*total-variogram effect*'. This measure of input importance encapsulates sensitivity information across the full spectrum of perturbation scales; see *Razavi and Gupta (2016a)* and *Haghnegahdar and Razavi (2017)* for further details.

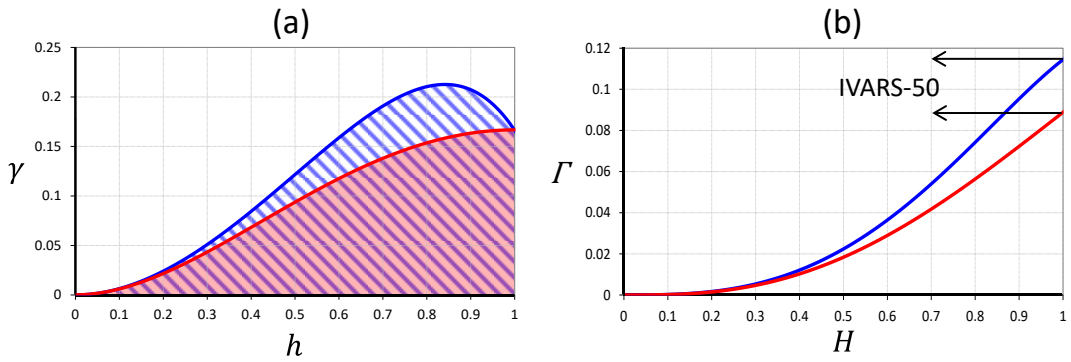

Figure 1. Illustrative example of (a) directional variograms and (b) integrated variograms for a hypothetical model with only two inputs. This example is adopted from Example 1a of Razavi and Gupta (2016a), where the range of inputs (θ) is two, resulting in a range of perturbation scales (h) of one, which is half of the input range.

Various studies have been shown VARS to be highly efficient and statistically robust (e.g., *Razavi and Gupta, 2016b; Alipour et al., 2022; Becker, 2020*). This efficiency is partly attributed to the estimation method used to calculate directional variograms, which relies on pairs of sample points rather than individual sample points (*Razavi and Gupta, 2016a & b*), thereby exploiting the fact that the number of pairs grows geometrically with an increase in the number of samples. As a result, VARS has been proven capable of effectively accommodating high-dimensional problems (*Sheikholeslami et al., 2019*). In the following sub-section, we expand upon this framework to adapt it for use in the context of XAI.

2.2. VARS with complex input distributions

A vast majority of SA methods and their applications in the literature operate under the assumption that model inputs are independent and uniformly distributed (*Do and Razavi, 2020*). This simplifying assumption is often made for the sake of computational convenience, as (1) accurately characterizing the multivariate distribution of inputs can be challenging or impractical in many cases, and (2) even if such distributions exist, incorporating them into the analysis may introduce computational complexity or feasibility issues. To address these limitations, Do and Razavi (2020) developed *Generalized VARS* (G-VARS), one of the first SA methods capable of accommodating correlated inputs.

G-VARS involves novel sampling and estimation strategies that map the original input space onto a standard normal space, while accounting for pair-wise correlations between inputs using the *Nataf Isoprobabilistic Transformation*. However, G-VARS is constrained to handling simple, theoretical

multivariate distributions such as normal and triangular distributions. While these distributions can be quite effective in characterizing various variables in modeling exercises, such as the parameters of a hydrologic model as demonstrated by *Do and Razavi (2020)*, they may offer limited assistance in characterizing highly complex datasets typical of ML inputs.

Figure 2 shows an illustrative three-variable example of datasets commonly encountered in practice. The marginal distributions of real-world variables (e.g., Figure 2a) may be quite complex, exhibiting features such as multiple modes, discontinuities, and long or heavy tails, while potentially being correlated with one another (e.g., Figures 2b-c). Approximating such complex multivariate distributions with classic theoretical distributions can often prove infeasible or impractical. Here, we developed a mathematical construct, called G-VARS2, that adopts an *empirical* approach to represent the marginal distributional properties of the data, as detailed below.

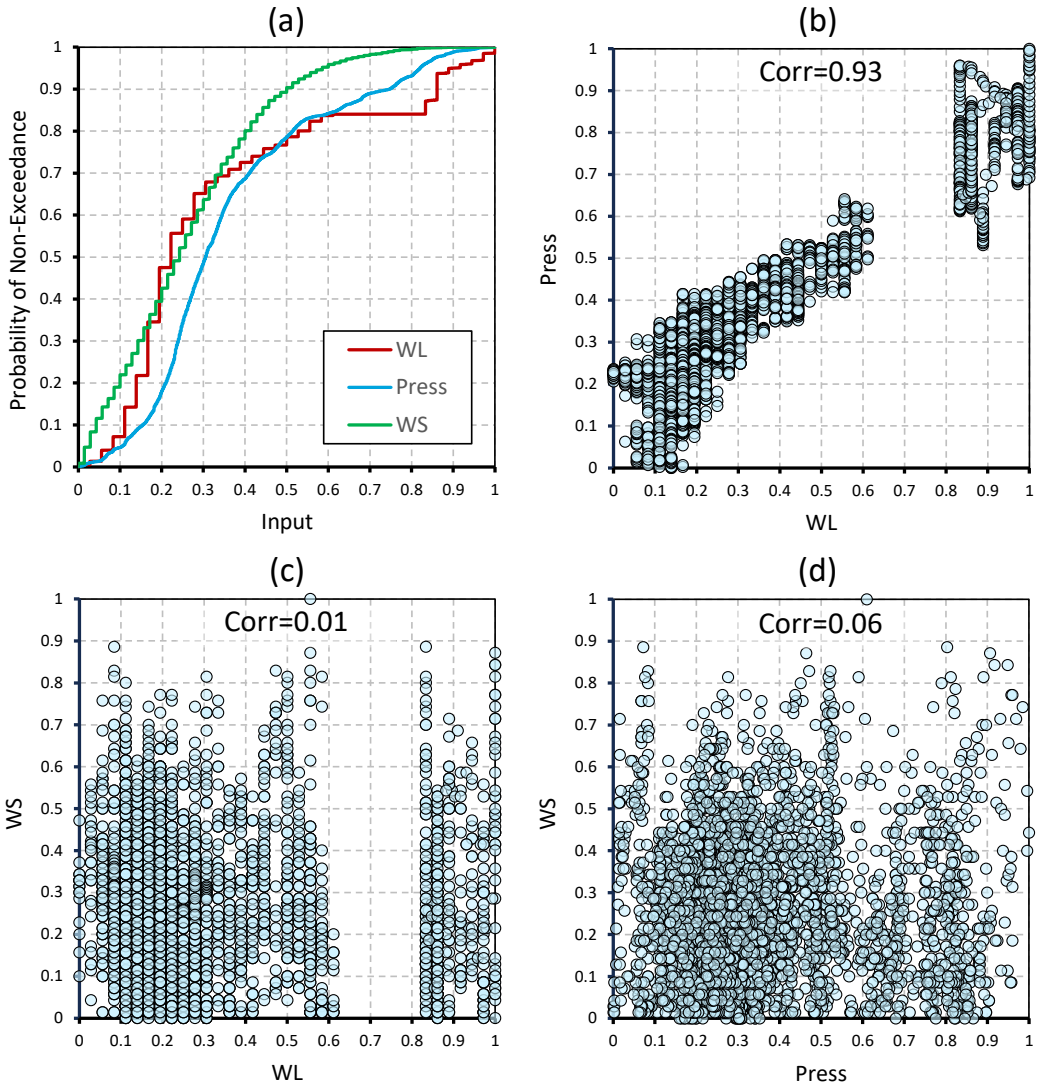

Figure 2. Example datasets used as inputs in machine learning. (a) Marginal cumulative distribution functions (CDFs). (b-d) Scatter plots and Pearson correlation coefficients (Corr) of pairs of inputs. WL, Press, and WS stand for water level, water pressure at the sediment-water interface, and wind speed, respectively. The data shown are from the case study described in the next section.

Suppose a model receives a set of n inputs, $\boldsymbol{\theta} = \{\theta_i \text{ for } i = 1, \dots, n\}$, that follow a multivariate distribution, $p(\boldsymbol{\theta})$, and produces an output, $Z(\boldsymbol{\theta})$. Let $\boldsymbol{\theta}_{\sim i}$ denote the set of all inputs except θ_i, and θ_i' denote $\theta_i + h_i$, where h_i is a perturbation to θ_i. Now, Equation (1) can be rewritten as:

$$\gamma(h) = \frac{1}{2} V\left[Z\left(\theta_i' \mid_{\boldsymbol{\theta}_{\sim i}}, \boldsymbol{\theta}_{\sim i}\right) - Z\left(\theta_i \mid_{\boldsymbol{\theta}_{\sim i}}, \boldsymbol{\theta}_{\sim i}\right)\right] \quad (3)$$

where $\boldsymbol{\theta}_{\sim i}$ follows $p(\boldsymbol{\theta}_{\sim i})$, which is the marginal distribution derived from $p(\boldsymbol{\theta})$, and where $\theta_i' \mid_{\boldsymbol{\theta}_{\sim i}}$ and $\theta_i \mid_{\boldsymbol{\theta}_{\sim i}}$ follow the conditional distributions when the inputs $\boldsymbol{\theta}_{\sim i}$ are set at specific values. Following the proof in *Razavi and Gupta (2016a & b)*, the above equation can be numerically approximated by sampling pairs of points from the model input-output space:

$$\hat{\gamma}(h_i) = \frac{1}{2N_h} \sum_1^{N_h} \left[Z\left(\theta_i' \mid_{\boldsymbol{\theta}_{\sim i}}, \boldsymbol{\theta}_{\sim i}\right) - Z\left(\theta_i \mid_{\boldsymbol{\theta}_{\sim i}}, \boldsymbol{\theta}_{\sim i}\right)\right]^2 \quad (4)$$

where N_h is the number of pairs of samples, spaced h_i apart, in the direction of θ_i.

Here, we adjust the sampling method of *Do and Razavi (2020)* to accommodate any 'custom' marginal distribution of $p(\boldsymbol{\theta})$ that may exist in real-world data. The new method utilizes any available sample of data for individual inputs to construct their empirical distributions, by calculating the frequencies of different values or ranges of values from the data sample. Empirical distributions provide a data-driven summary of the observed data's distributional properties when the underlying theoretical distribution is unknown, or is difficult to model accurately.

The new method processes a data sample for each input θ_i to derive its cumulative distribution function (CDF) through the *Weibull* empirical approach, by sorting data entries in ascending order and assigning each entry a probability of non-exceedance. Subsequently, the actual CDF of input θ_i, denoted as F_{θ_i}, is estimated by linearly interpolating the points on the respective empirical CDF. The lower and upper bounds of a custom-distributed input are assumed to be the minimum and maximum values of the corresponding sample. Next, the inverse of F_{θ_i} for all inputs ($F_{\theta_i}^{-1}$) is incorporated into the G-VARS framework through the following equation:

$$\theta_i = F_{\theta_i}^{-1}[\phi(X_i)] \quad (5)$$

facilitating the transformation of samples between a standard normal space $\boldsymbol{X} = \{X_i \text{ for } i = 1, \dots, n\}$ and the original input space $\boldsymbol{\theta}$, where $\phi(.)$ denotes the theoretical CDF of a standard normal distribution. The software developed for G-VARS2 is accessible on GitHub at the following link: *https://github.com/vars-tool/vars-tool*.

3. Data used in ML: Pilot Scale Pit Lake

In the *Athabasca Oil Sands* (AOS) region of *Western Canada*, the accumulation of fluid tailings (FT) and Oil Sands Process affected Water (OSPW) in tailing ponds has reached a concerning level that has attracted global attention (*Gosselin et al., 2010; AEP, 2015; McNeill, 2017*). Despite decades of research on several experimental reclamation techniques for fluid tailings management in the oil sand regions (*COSIA, 2012*), there is still a need for an advanced pit lake technology under water capped fined deposit to handle the substantial amount of FT (*Cossey et al., 2021*). To address this, one company in the AOS industries has developed a pilot-scale experimental pit lake called *Lake Miwasin* as a prototypic precursor to large end pit lakes.

Extensive measurements of water quantity and quality variables have been ongoing since the construction of the lake to evaluate the performance of the system over time and its effectiveness in reclaiming significant quantities of treated tailings materials stored onsite at the AOS. Our group has been using wireless sensor technology to monitor water quality parameters at a high measurement frequency, to

gain a deeper understanding of the system's functioning, and to help guide further development and use of pit lake strategies to mitigate the negative impacts of fluid waste on the environment.

Located on the east side of the *Athabasca River* (56º 53' 14" N and 111º 23' 7" W), Alberta, Canada, *Lake Miwasin* is an engineered water body constructed using oil sand by-products as bottom substrate (TFT) and overlying water (OSPW). The lake measures 70 m in width, 165 m in length and reaches a maximum water depth of around 4.5 m. A littoral zone in the lake, comprising approximately 20% of the water surface area, is present along the eastern periphery. This zone features a 0.2-5% slope that extends into the surrounding upland, where limnetic zone has deep depth with substantial bottom substrate.

The wireless sensor network (WSN) was employed in both littoral and limnetic zones of the lake to monitor (hourly) and relay information on key water quality parameters. The *Lake Miwasin* WSN utilized the *Libelium*^{TM} smart water extreme and smart water ion models for monitoring. The sensor probes were calibrated with standard solutions from *Libelium* (*Libelium, 2020*). Data was transmitted directly from the sensor device to cloud storage through the *ThingSpeak*^{TM} *Cloud* service and mobile devices using the local 4G network (via mobile SIM card). The sensor units, housed in custom acrylic boxes (30 × 25 × 25 cm) for protection against field conditions, were affixed to high-density Styrofoam platforms (60 × 60 × 5 cm for each sensor unit) using cinderblock anchors (Figure 3). Figure 3a illustrates one-time introduction of TFT and OSPW stemming from the oil sands mining and extraction processes, Figure 3b shows contemporary methods employed for treatment and reclamation of fluid tailings within AOS region, and Figure 3c shows WSN technology was deployed in Lake Miwasin to monitor the water quality conditions of the lake as the lake system ages.

Before deployment at *Lake Miwasin*, a similar WSN methodology was tested in Canadian lakes to delineate effluent exposure downstream of a Uranium Mill region (*Cupe-Flores et al., 2022*) and to estimate selenium (Se) exposure using a site-specific threshold value (*Peixoto Mendes et al., 2023*). In *Lake Miwasin*, deployment spanned from September 18th to October 10th in 2020; and from June 21st to October 16th in 2021. Coinciding with visits to the lake for probe maintenance, we collected water samples at each station, twice in 2020 and six times in 2021. For validation of sensor reading, samples were collected manually in two replicates for each monitoring depth approximately 5 to 10 m apart from probes using a Wildco® 2.2-L acrylic Van Dorn horizontal beta water sampler (Wildlife Supply, USA).

Prior to sampling, the sampler was thoroughly rinsed with lake surface water to avoid cross-contamination between different station zones. The water sample was placed into pre-acid-washed ~250 mL and 30-ml high-density polyethylene *Nalgene*^{TM} bottles (prewashed with 10% nitric acid and rinsed with distilled water). Subsequently, the 30mL bottle samples were filtered through a 0.45-µm polyether sulfone membrane into two sets of 10mL high-density polyethylene *Nalgene*^{TM} bottles using 5-ml syringes. Then samples were refrigerated and transported in an ice-packed cooler to the *University of Saskatchewan Toxicology Centre* (Saskatoon, SK, Canada) and kept at 4°C until laboratory analysis. A *Thermo Scientific™ Orion Star™ A329* portable multiparameter meter (Thermo Fisher Scientific, USA) was used to measure in situ parameters (pH, EC, temperature, and DO) at a pre-defined monitoring depth. Similarly, the turbidity was measured with a calibrated bench top turbidity meter (LaMotte®, 2020 meter). Field blanks containing distilled water were included during sampling for quality control. Water quality parameters measured by the sensor probes by our research team at University of Saskatchewan.

Additional climatological parameters included in this study were collected by Suncor Energy Inc. from the meteorological station installed at the lake. In the context of studying this lake system, the focus was on predicting key water quality parameters through the application of kernel-based, connectionist models, and ensemble tree-based ML techniques.

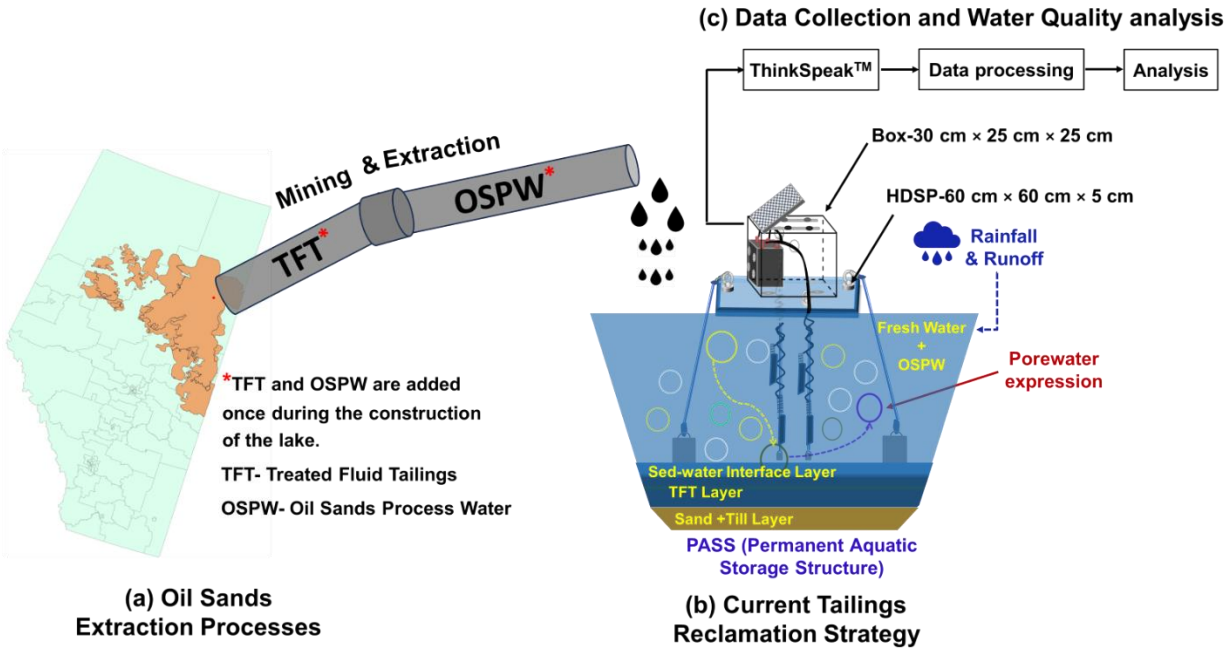

Figure 3. Graphical description of elements used for characterizing key water quality parameters in Lake Miwasin.

4. Design of Experiments

We evaluated the proposed SA method (G-VARS2) across various ML models, encompassing tree-based, connectionist, and kernel-based models. Our objective was to gauge the robustness and consistency of these models and to glean insights into controlling variables in the prediction process. This experiment allowed us to not only develop accurate predictive ML models but also to provide transparent and interpretable explanations regarding the inputs driving the predictions made by these models (Figure 4). Similar to G-VARS, the user of G-VARS2 must set the following two algorithm parameters for sampling and estimation: the number of star centers and the number of cross-sectional points. For this study, we selected 100 and 10 for the former and latter, respectively. The selection of these numbers was informed by our prior experience, and they have consistently shown robustness and stability in our initial evaluations.

The tree-based ML models we used here include classic decision trees (DT), bagging-based random forest (RF; *Breiman, 2001*), and boosting models including adaptive boosting (AdaBoost; *Freund and Schapire, 1997*), gradient boosting (GBoost; *Friedman, 2001*), extreme gradient boosting (XgBoost; *Chen and Guestri, 2016*), and light gradient boosting (LgBoost; *Ke et al., 2017*). Further, we used two artificial neural networks (ANNs), one with a shallow, single hidden layer (ANN-S) and another with a deeper architecture (ANN-D), and two support vector regression (SVR) models, one with default (DSVR) and another with tuned parameterization (TSVR) (Table S1). We also used multiple linear regression (LR) to provide a minimalist performance as a benchmark for model comparison.

We chose to assess the above ML models (Figure 4b) because they have been used widely in the realm of surface water quality modeling (*Palani et al., 2008; Ahmed, 2014; Najah et al., 2014; Ahmed et al., 2019a; Ahmed et al., 2019b; Abobakr Yahya et al., 2019; Banerjee et al., 2019; Sinshaw et al. 2019; Zou et al., 2019; Barzegar et al., 2020; Yim et al., 2020; Khullar and Singh, 2021; Yamamoto et al., 2021; Zhang et al., 2021; Zhou and Zhang, 2023*). Moreover, there is a growing literature on the application of advanced

bagging-boosting ensemble models based on DT in environmental sciences. These applications include estimating crop yields (*Liakos et al., 2018*), assessing energy performance (*Wang et al., 2018*), predicting water demand (*Wang et al., 2014*), estimating air particulate levels (*Brokampet et al., 2018*), quantifying climate and catchment control on hydrological drought (*Konapala and Mishra, 2019*), creating susceptibility maps for gully erosion (*Rahmati et al., 2017; Garosi et al., 2019*), mapping groundwater yield (*Sameen et al., 2019; Jeihouni et al., 2020; Mosavi et al., 2021*), predicting solar and wind energy (*Torres-Barrán et al. 2019*), forecasting water usage and rainfall (*Kim et al., 2020*). Although bagging-boosting models hold significant promise, their utilization in surface water quality research remains relatively limited (*Chen et al., 2020*). Examples include predicting biological oxygen demand, chemical oxygen demand (*Khullar and Singh, 2021*), turbidity (*Zhang et al., 2021*), Chlorophyll-a (*Savoy and Harvey, 2023*) and other water quality parameters such as permanganate index (COD_{Mn}), total phosphorus (TP), and total nitrogen (TN) (*Wang et al., 2021*), dissolved oxygen (DO), and ammonia (NH_3-N) (*Chen et al., 2020*).

In our analyses, we further accounted for the impact of data-splitting for training and testing of the different ML models as well as randomization in initializing the ML models. This is a very important, but often neglected step in model development, as described in *Maier et al. (2023)*. To do so, we developed 30 replicates of every ML model (Figure 4c), each with a different random seed number for data-splitting and model initialization (Table S1). The detailed default and tuned hyperparameter values for all the ML models are presented in Table S2. We employed a standard approach to partition the datasets into two subsets for each ML model: 70% for the training dataset and 30% for the testing dataset. During the development phase, the training dataset was utilized as the foundation for constructing models, while the testing dataset served the critical role of evaluation by enabling performance comparisons among the developed models. The normalization and minimum-maximum scaling of all input and output variables were performed using the scikit-learn pre-processing library in Python (*Pedregosa et al. 2011*).

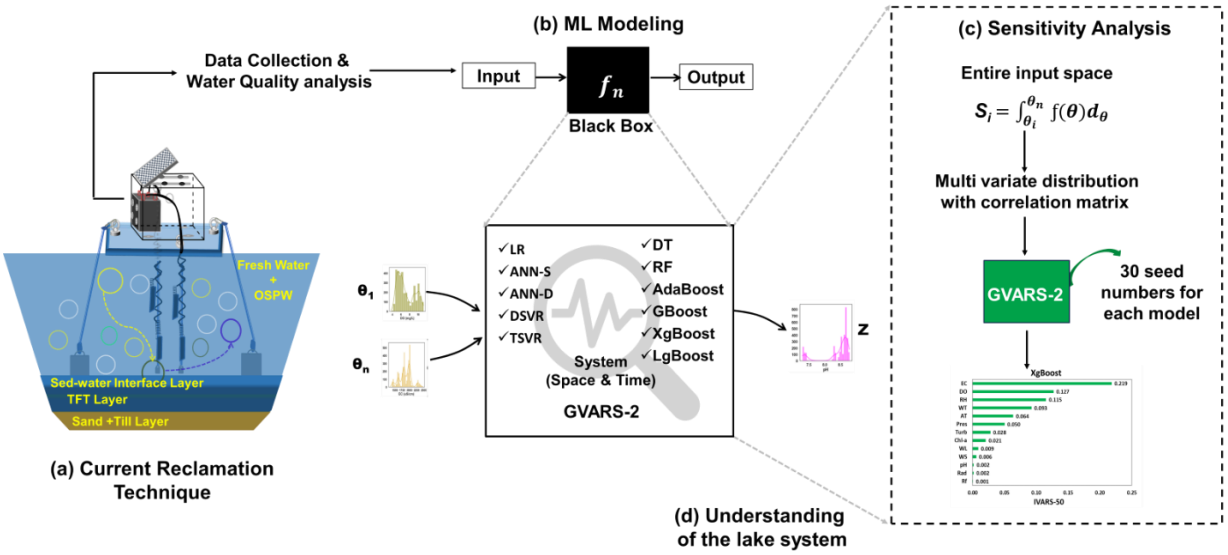

Figure 4. An illustration of the workflow, spanning from sampling to machine learning (ML) modeling, and subsequently to sensitivity analysis (SA). LR: Linear Regression; ANN-S: Simple Artificial Neural Network; ANN-D: Deep Artificial Neural Network; DSVR: Default Support Vector Regression; TSVR: Tunned Support Vector Regression; DT: Decision Tree; RF: Random Forest; AdaBoost: Adaptive Boosting; GBoost: Gradient Boosting; XgBoost: Extreme Gradient Boosting; LgBoost: Light Gradient Boosting.

To gauge the accuracy of our ML-based water quality prediction models, we utilized two performance metrics: the coefficient of determination (R^2) and the root mean squared error (RMSE) as follows:

$$R^2 = \left(\frac{\sum_{i=1}^{n}[(O_i - \bar{O})(P_i - \bar{P})]}{\sqrt{[(\sum_{i=1}^{n}(O_i - \bar{O})^2)(\sum_{i=1}^{n}(P_i - \bar{P})^2)]}} \right)^2 \quad (6)$$

$$RMSE = \sqrt{\frac{1}{n}\sum_{i=1}^{n}(O_i - P_i)^2} \quad (7)$$

where O_i and P_i are the observed and predicted values, respectively, $\bar{O}$ and $\bar{P}$ are the mean of the observed and predicted values, respectively, and *n* is the number of data points.

Water quality monitoring in *Lake Miwasin* at the SWI involves collecting, measuring, and analysing water samples to understand their chemical and biological attributes (*Sinshaw et al. 2019*). We used the following sensor measured water quality variables: dissolved oxygen concentration (DO), pH, water temperature (WT), conductivity (EC), chlorophyll-a (Chl-a), turbidity (Turb), ammonium (NH_4^+).We also used meteorological variables, including water level (WL), wind speed (WS), solar radiation (Rad), water pressure (Press), air temperature (AT), rainfall (Rf), relative humidity (RH). Using these variables, we constructed ML-based models to predict four key water quality variables—NH_4^+, Chl-a, DO, and pH—utilizing all other variables as predictors (see summary statistics in Table S3). The selected target variables are pivotal for lake monitoring, as they play a fundamental role in assessing the health of aquatic ecosystems, influencing the growth and respiratory capabilities of aquatic life (*Wetzel, 2001; Sánchez et al., 2006; Pena et al., 2010; Risacher et al., 2018; Barzegar et al., 2020*). Moreover, these variables provide decision-makers with vital data to address environmental challenges in a sustainable manner (*Wu and Liu 2012; Wu and Chen, 2013*).

5. Results and Discussion

This section presents the outcomes of the designed experiments aimed at evaluating and explaining the performance of various ML models using the developed SA method. We structure the results and discussion around four key questions: (1) What is the predictive efficacy of different ML models? (2) Which physico-chemical variables influence the predictions of ML models? (3) How robust and consistent is the explanatory power of different ML models? (4) What novel insights do the ML models offer into the underlying physico-chemical processes?

5.1. What is the predictive power of different ML models?

Figure 5 illustrates the predictive performance of various ML models across different target variables during both the training and testing phases. Generally, these models demonstrated robust predictive capabilities for pH, ranking second in performance for dissolved oxygen (DO), while exhibiting relatively lower accuracy for predicting NH_4^+ and chlorophyll-a (Chl-a) levels. Notably, all ML models achieved satisfactory performance for pH (with $R^2 > 0.93$ for linear regression (LR) and > 0.98 for other ML models) and DO ($R^2 > 0.86$ for LR and > 0.9 for others). The LR model could only provide satisfactory performance in the case of pH and DO prediction, suggesting that predicting NH_4^+ and Chl-a concentrations in the lake rely predominantly on non-linear relationships, surpassing the capabilities of the LR model.

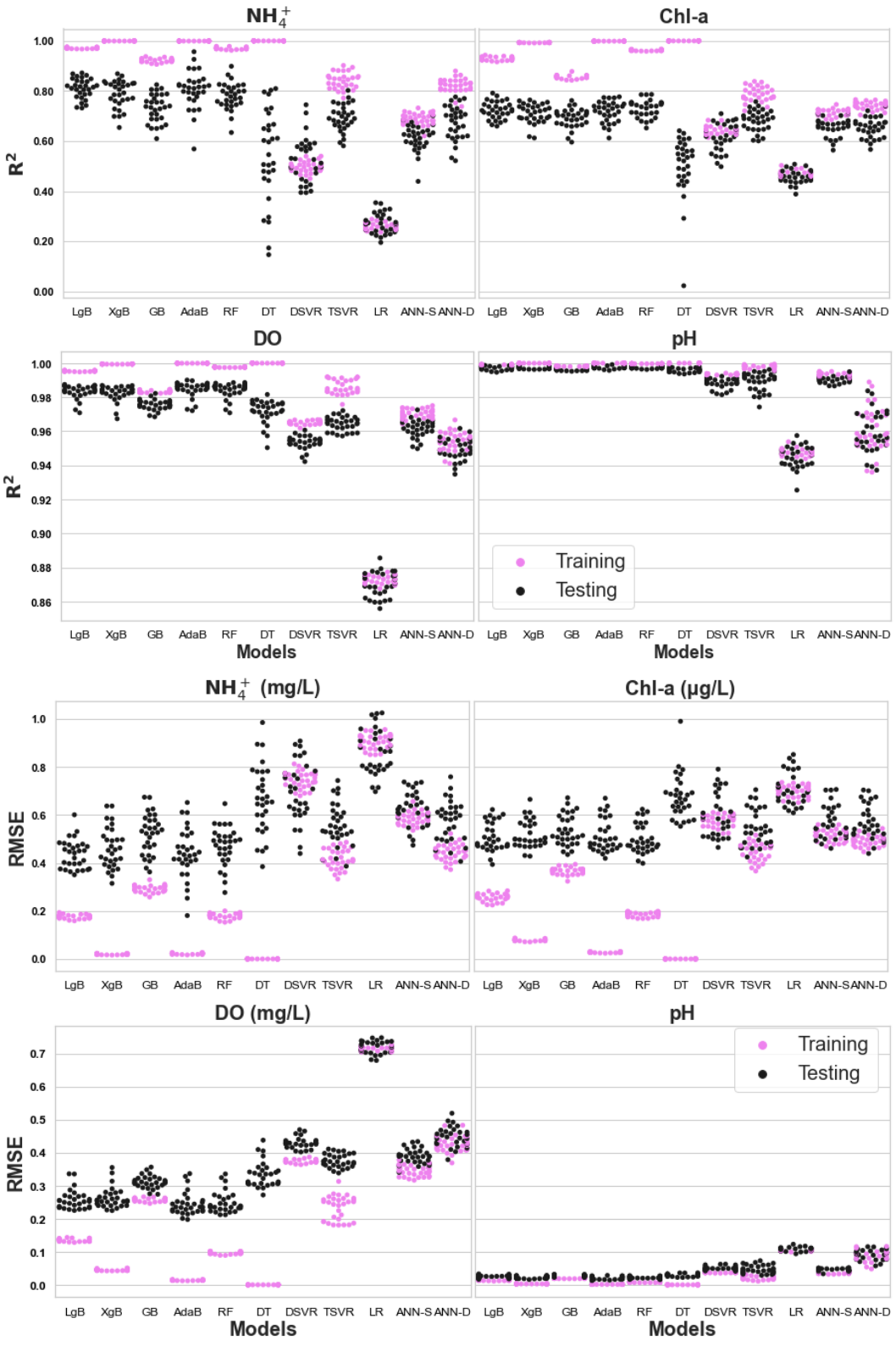

Figure 5. Performance of different ML models in training and testing across 30 replicates, each with a different random seed, according to the coefficient of determination (R^2) and root mean squared errors (RMSE). LgB: Light Gradient Boosting; XgB: Extreme Gradient Boosting; GB: Gradient Boosting;

AdaB: Adaptive Boosting; DT: Decision Tree; DSVR: Default Support Vector Regression; TSVR: Tunned Support Vector Regression; L: Linear Regression; ANN-S: Simple Artificial Neural Network; ANN-D: Deep Artificial Neural Network.

The results show that tree-based ML models outperformed the connectionist and kernel-based ML and basic decision tree (DT) models. Throughout training, all tree-based models achieved R^2 scores remarkably close to one. However, their performance declined notably on testing datasets (considerable reduction in performance), particularly in NH_4^+ and Chl-a predictions. Importantly, all tree-based models with default hyperparameter settings demonstrated acceptable performance, alleviating the need for extensive hyperparameter tuning. This underscores the efficacy of these models in providing accurate predictions for lake variables, albeit with some limitations in predicting certain parameters under testing conditions.

The variations observed in model performance depicted in Figure 5 across diverse seed numbers primarily stem from the intrinsic randomness inherent in the model training processes, functional classes, and data splitting. This susceptibility to initial conditions is a common trait among the ML models employed in this study. For instance, the connectionist models such as ANN-S and ANN-D are influenced by variation in the initial weights associated with different seeds, while variations in kernel-based SVR arise due to different support vectors chosen in each model replicate. The basic DT model exhibits large variability in testing due to the diverse tree structures resulting for different data splits. However, the ensemble tree-based models such as bagging and boosting models were able to reduce those variations by building multiple DTs and aggregating their predictions.

Another notable observation is the large reduction in model performance from training to testing for certain models, particularly DT, AdaBoost, and XgBoost, underscoring the importance of thorough testing and evaluation on datasets not utilized in training. More broadly, comprehending and addressing potential variations in model performance resulting from various factors is crucial for recognizing the uncertainty associated with the outcomes of ML models. The findings from the application of the proposed SA-based method can provide further insights into this issue, as detailed in the subsequent sections.

5.2. What physico-chemical variables control the predictions of ML models?

Most of the ML models showed success in mapping the inputs to the outputs in the pit lake, albeit to varying degrees. In addition to providing predictive ability, these input-output mappings can potentially offer a wealth of information on how the underlying physico-chemical processes work. However, such mappings are typically comprised of very complex relationships that are hard to understand and explain. Accordingly, use of SA to interrogate the ML models helps in characterizing the importance of the different inputs on the functioning of the models to produce the output. Note that the SA method was run on each of the 30 replicates of every ML model for each target output.

In Figure 6, star plots are to illustrate the overall importance (average over 30 replicates) of the inputs into each of the ML models. The further a spoke extends outwards within the circle, the more influential the respective input is in predicting the output. Accordingly, Rad and RH were identified as the most influential inputs to the connectionist and kernel-based models for the predictions of NH_4^+ and Chl-a, respectively. In contrast, for the tree-based models, DO and pH respectively turned out to be the most influential inputs for prediction of NH_4^+ and Chl-a. For prediction of DO and pH, the connectionist and kernel-based models were more sensitive to Rad, AT, and RH. The tree-based models, however, were more sensitive to NH_4^+, pH and Chl-a for the prediction of DO and to WL, WT and NH_4^+ for the prediction of pH.

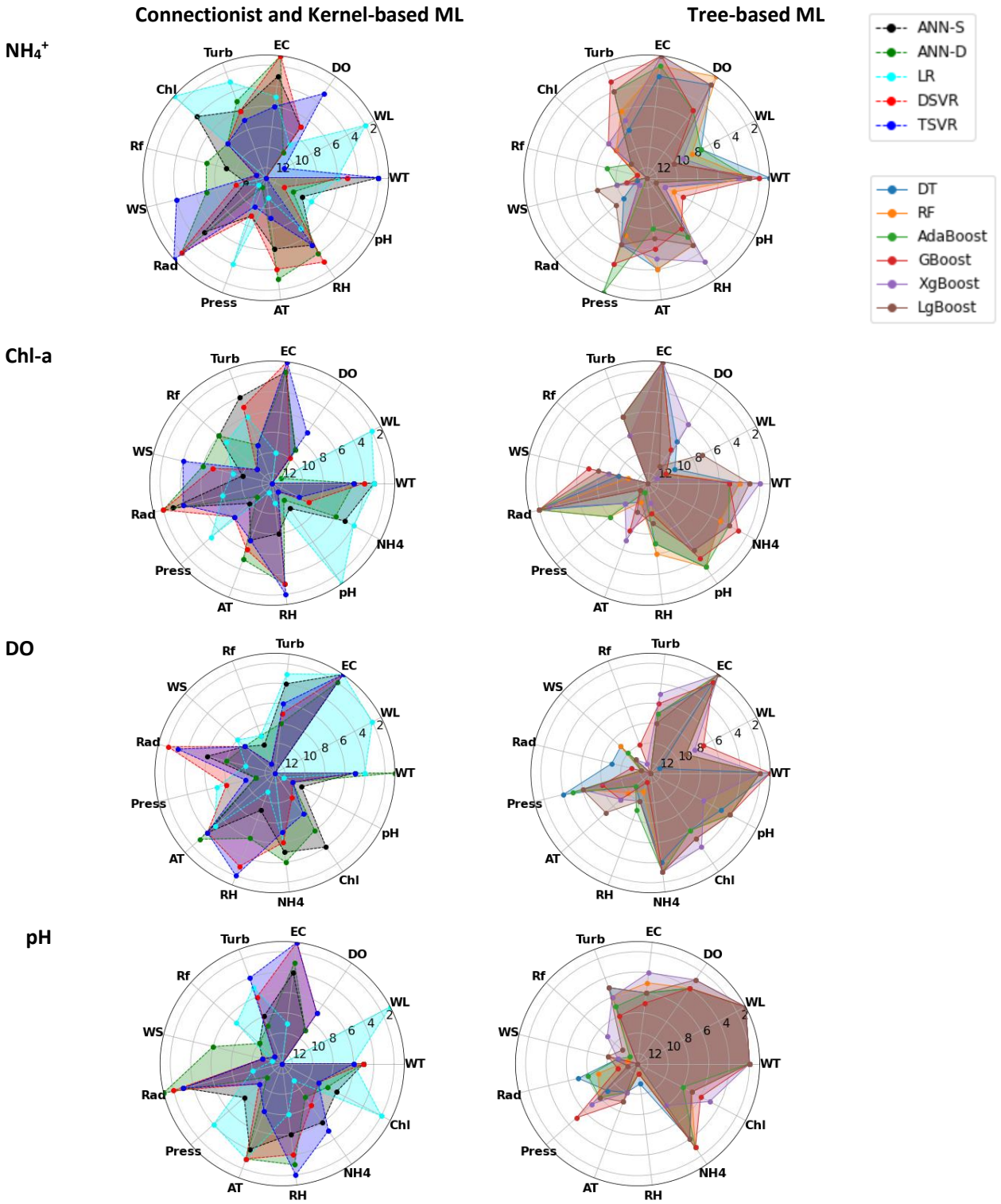

Figure 6. Input importance of different ML models (connectionist and tree-based) characterized through the proposed sensitivity analysis that is based on Integrated Variogram Across a Range of Scales (IVARS-50). Shown for each ML model is the median of input rankings across the 30 replicates. Rank 1 indicates the most influential input, rank 2 the second most influential input and so on.

Furthermore, the importance of some inputs turned out to be quite different in the case of different ML models. For example, EC was identified to be the most important input by DSVR to predict NH_4^+, 3rd most important by ANN-S, and the 7th most important by TSVR. Moreover, the rankings based on the linear regression model were largely inconsistent with those based on other models, suggesting the existence of strong non-linearity in the problems at hand. Overall, such considerable differences in input variable importance indicate that, while different ML models may show comparable performance in terms of predictive power, they may do so by relying on entirely different signals embedded in the training data (Figures S1-S4).

We should note that prior to doing any modeling we observed from histogram plots and correlations that water quality parameters such as conductivity (EC), Total Dissolved Solids (TDS), and Salinity have very similar data distributions and are highly correlated (*~0.99*). A similar pattern was observed for DO and Saturated oxygen concentration. If not addressed, this high level of correlation can lead to what is known as "*substitution effects*," where different variables can essentially serve as substitutes for each other in explaining the outcome. To tackle the problem of collinearity in the input dataset, we selected only EC and DO to use as inputs and discarded the parameters that were highly correlated to them, finally retaining only a few of the parameters (pH, Press and WL) that had a moderately high correlation of *~0.90*. This choice to retain EC and DO is based on existing theory in the AOS region. It is worth noting that the discarded parameters were computed empirically by the WSN system.

Note, however, that the novel reclamation technique being used in Lake Miwasin ages over time, causing the lake to differ from its natural state in various ways, so we cannot solely rely on existing scientific evidence. Moreover, our ML models, particularly RF and all Boosting models inherently address substitution effects through regularization and ensemble techniques. Further, the various ML models differ in their choice of explanatory variables, which is relevant to understanding these substitution effects. Certain ML strategies are more susceptible to this issue while others are not when selecting explanatory variables.

5.3. How robust is the explanatory power of different ML models?

By robustness, we refer here to low sensitivity of the ML results to the random seed chosen for the randomization of their initial weights and for the splitting of available data to training and testing subsets. Overall, the results of a more robust model are expected to be more reliable, particularly in the cases where available data are limited. Here, we assessed model robustness by checking the dispersion of SA results across 30 replicates. The more dispersed the input importance is across replicates, the less robust is the model. Figure 7 shows the distribution of input ranks as perceived by different ML models across the 30 replicates in predicting DO. Overall, the ANN-based models demonstrated the lowest robustness, frequently relying upon different inputs as their primary controls for driving an output.

For example, ANNs showed a wide range of sensitivity to WT, Turb, and Chl when predicting DO, almost as if the model may randomly pick up different predictive signals in the data each time it is set up. The level of robustness demonstrated by ANN-D may be deemed comparable to that of ANN-S, although they showed different predictive power in the previous sub-section. On the other hand, some ML models showed high robustness, consistently identifying the same/similar inputs as their primary drivers for prediction. For example, the variants of gradient boosting, such as GBoost, XgBoost and LgBoost models, show comparatively less dispersion in behaviour over the 30 replicates, indicating more consistency in their results.

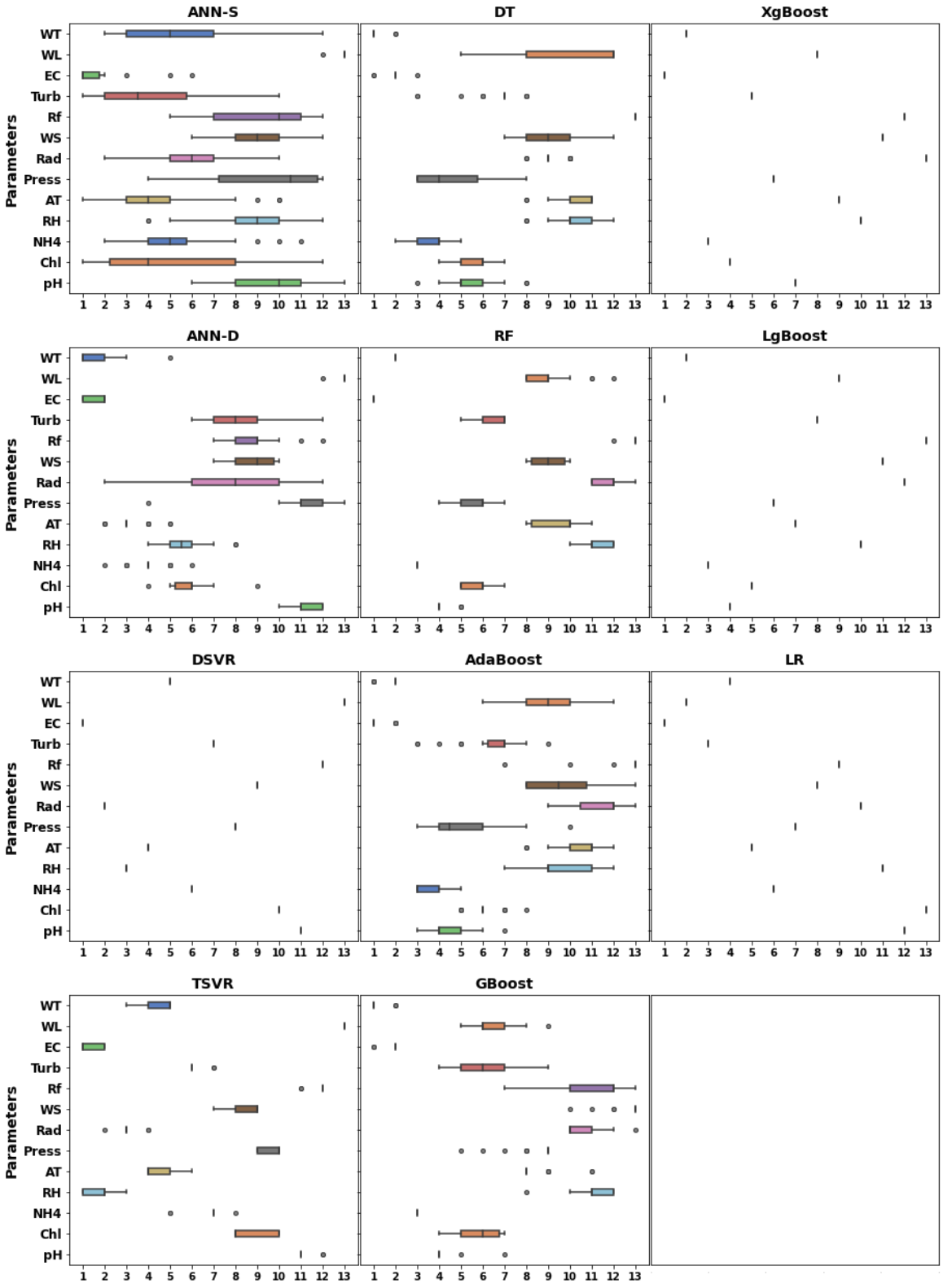

Figure 7. Box plots showing the dispersity (range and distribution) of input importance for DO across the 30 replicates; Rank 1 indicates the most influential the respective input.

In general, the boosting models yielded very similar sets of "*most influential*" inputs but with slightly different orders in their ranking. AdaBoost was an exception, showing large variability in rankings, due to its random weight initialization process for model training. An interesting observation was the behaviour of support vector regression with default hyperparameters (DSVR) versus that with hyper-parameter tuning (TSVR). The former showed no variability in input rankings, while the latter showed some level of variability due to hyperparameter tuning separately for each of the 30 replicates. This indicates that the robustness of an ML model may be partly a manifestation of its inherent mechanisms in fitting data, and partly of the way the user sets them up. Figure S3 in supplementary materials shows similar results for ML models predicting the other target variables.

5.4. What new insights do the ML models provide into the underlying physico-chemical processes?

The SA-based explanation approach assessed the extent to which one variable can be impacted by other variables, with the strength of these influences reflecting the underlying physical processes in *Lake Miwasin*. Here, we compare the ML results for predicting NH_4^+, Chl-a, DO and pH with established scientific evidence from the oil sands region, primarily drawn from literature reviews and our research background. By answering this research question, our objective was to highlight the explanations provided by ML models that align with conventional wisdom and those that do not. Of course, it is always possible that some new explanations may be discovered that identify relationships we are either unaware of or that are not recognized by existing theories. This exploration may yield two possible scenarios, one where the ML model may be providing the right answer for wrong reason and another where it challenges the validity of existing theory.

From the SA results, we see that NH_4^+ concentrations at the sediment water interface in the lake are influenced by parameters like EC, WT, AT, DO, turbidity, and Press (as seen in Figure 5). The water content present in parent untreated fluid tailings contains high concentrations of dissolved constituents, including Na, Cl, organics, and NH_3 (*Dompierre et al., 2016*). These dissolved constituents are released from tailings due to the upward movement of water associated with tailings densification (*Dompierre and Barbour 2016*), providing a mechanistic explanation for the associations between EC and NH_3 (detectable NH_4^+). AT affects WT, which in turn influences the rate of microbial respiration, with elevated WT promoting biological oxygen demand and production of NH_3 (*Stumm and Morgan, 2012*). Warmer temperatures and declining DO can also increase sediment bioturbation rate by chironomid (invertebrate) larvae (*Roskosch et al., 2012*), further promoting bio-irrigation-mediated benthic fluxes of salt, NH_3, and other dissolved constituents.

Further, there is an interplay between NH_4^+ and DO, as NH_4^+ could be an oxygen consuming constituent in oil sands end pit lakes (*Risacher et al. 2018*). The DO parameter was well captured by the tree-based model, while the connectionist ML models were unable to identify DO as an important parameter for NH_4^+. Moreover, the interplay between overland water flow and bioturbation enhances metal flux from low permeability sediment beds (*Amato et al., 2016; Xie et al., 2018*). In particular, it is possible that this bioturbation process can partly destabilise the sediment bed in *Lake Miwasin* and cause a temporary remobilisation of suspended particles and particulate organic matter that can yield to overall fluctuation in turbidity levels. Fluid tailings is a source of particulate organic matter (*Sasar et al., 2022*) and may increase turbidity values during periods of water column stratification. Overall, the influential input parameters (EC, WT, AT, DO, Turb) are very well captured by tree-based models in our SA for prediction of NH_4^+.

The SA indicates that Chl-a prediction using ML models are mostly influenced by WT, EC, Rad (light), pH, NH_4^+. Evidence showed that Chl-a could be an indicator of (a) photosynthesis (affected by DO, solar radiation, and temperature; Shammas et al., 2009; Wallace et al., 2016); (b) nutrient status (affected by pH since algae grow better at higher pH values by taking up more nutrients and CO_2 under alkaline

conditions; *Veeresh et al., 2010; Wallace et al., 2016*), and (c) the growth and distribution of phytoplankton species composition (affected by solar light, DO and WT; *Harrison et al., 2018; Bouffard et al., 2018, Liu and Georgakakos, 2021*) in the lake. Without any ambiguity, our SA method captured most of the important sensitive parameters for Chl-a prediction using the tree-based models, but it failed to identify DO as an important input.

For prediction of DO, the suggested variables EC, WT, NH_4^+, and pH are frequently signaled by different models in the SA. Similarly, the prediction of pH can be influenced by WL, WT, NH_4^+, and DO (Figure 6). Most of these parameters are indirectly or directly involved in different processes occurring within the lake, such as release of pore water from TFT and fluctuation of DO due to the release of oxygen consuming constituents (e.g., NH_4^+) (*Dompierre and Barbour, 2016; Risacher et al. 2018*). Based on our SA, the tree-based models identified most of these as sensitive parameters for prediction of DO and pH whereas the connectionist ML models did not (Figure 6).

6. Conclusions

This study developed a new approach to XAI through the lens of SA. This approach has the conceptual strength that it characterizes the entire response surface of an ML model – whereas other methods typically look only at the model response in the region of the available input-output data points. This approach was used to investigate the primary controls on the physico-chemical processes of a major environmental problem, as determined by a suite of connectionist, kernel-based, and tree-based ML models. The analyses enabled efficient detection of important explanatory variables, thereby guiding long-term monitoring programs with reduced data collection cost.

Notably, although most of the ML models showed similar levels of predictive power, they tended to base their predictions on different explanatory variables (inputs). In particular, the connectionist ML models such as neural networks showed a large degree of variability in how their outputs depended on the various inputs. Different replicates of the same connectionist model were often primarily driven by different inputs, suggesting that the model may pick up different signals in the data to provide similar levels of predictability. Interestingly, the important inputs of the tree-based ML models were more consistent with each other, while tending to be somewhat different from those of the connectionist and kernel-based models.

Overall, our analysis reveals an important issue that is arguably a critical takeaway message of this paper. Subtle alterations in the design of ML models (such as variations in the random seed used for initialization, functional classes, hyperparameters, or data splitting) can lead to entirely different representational interpretations of the dependence of the outputs on explanatory variables (inputs). This strongly reinforces the importance of utilizing ensembles of ML models when explanatory power is a desirable outcome (see also *De La Fuente et al., 2023*). Such ensembles could be generated via multiple replicates of the same model, or by employing diverse types of ML models, or some combination of both. Failure to do so could mean that the analysis cannot be relied upon to guarantee the delivery of robust and reliable predictions, particularly when using the developed models to generalize to conditions beyond the region(s) of the data used for model training.

Acknowledgement: We thank Suncor for their invaluable on-site assistance at Lake Miwasin and providing access to their database platform.

Funding: We acknowledge support by the Suncor Energy Inc.

Competing interests: The authors declare no conflict of interest.

Data and software availability: The software developed here for G-VARS2 has been made available on GitHub at *https://github.com/vars-tool/vars-tool*. The data used will be made available on a public repository.

REFERENCES:

Aas, K., Jullum, M., Løland, A. (2021). Explaining individual predictions when features are dependent: More accurate approximations to Shapley values. Artificial Intelligence, 298, 103502. https://doi.org/10.1016/j.artint.2021.103502.

AEP (2015). Total Area of the Oil Sands Tailings Ponds over Time, Oil Sands Information Portal, Alberta Environment and Parks, Edmonton, AB. Dataset no. 542. 4 March 2015. Available: http://osip.alberta.ca/library/Dataset/Details/542.

Abobakr Yahya, A. S., Najah, A., Othman, F. B., Ibrahim, R. K., Afan, H. A., El-Shafie, A., Fai, C. M., Hossain, M. S., Ehteram, M., & Elshafie, A. (2019). Water quality prediction model-based support vector machine model for ungauged river catchment under dual scenarios. Water, 11(6), 1231. https://doi.org/10.3390/w11061231.

Ahmed, A. A. M. (2014). Prediction of dissolved oxygen in Surma River by biochemical oxygen demand and chemical oxygen demand using the artificial neural networks (ANNs). Journal of King Saud University-Engineering Sciences, 29(2), 151-158. https://doi. org/10.1016/j.jksues.2014.05.001.

Ahmed, A.N., Othman, F. B., Afan, H. A., Ibrahim, R. K., Fai, C. M., Hossain, M. S., Hossain, M. S., Ehteram, M., & Elshafie, A. (2019a). Machine learning methods for better water quality prediction. Journal of Hydrology, 578, 124084. https://doi.org/10.1016/j.jhydrol.2019.124084.

Ahmed, U., Mumtaz, R., Anwar, H., Shah, A. A., Irfan, R., & García-Nieto, J. (2019b). Efficient water quality prediction using supervised machine learning. Water, 11(11), 2210. https://doi.org/10.3390/w11112210.

Alipour, A., Jafarzadegan, K., & Moradkhani, H. (2022). Global sensitivity analysis in hydrodynamic modeling and flood inundation mapping. Environmental Modelling & Software, 152, 105398. https://doi.org/10.1016/j.envsoft.2022.105398.

Amato, E. D., Simpson, S. L., Remaili, T. M., Spadaro, D. A., Jarolimek, C. V., & Jolley, D. F. (2016). Assessing the effects of bioturbation on metal bioavailability in contaminated sediments by diffusive gradients in thin films (DGT), Environ. Sci. Technol. 50(2016) 3055–3064. https://doi.org/10.1021/acs.est.5b04995.

Banerjee, A., Chakrabarty, M., Rakshit, N., Bhowmick, A.R., & Ray, S. (2019). Environmental factors as indicators of dissolved oxygen concentration and zooplankton abundance: Deep learning versus traditional regression approach. Ecological indicators, 100, 99-117. https://doi.org/10.1016/j.ecolind.2018.09.051.

Barzegar, R., Aalami, M. T., & Adamowski, J. (2020). Short-term water quality variable prediction using a hybrid CNN–LSTM deep learning model. Stochastic Environmental Research and Risk Assessment, 34(2), 415-433. https://doi.org/10.1007/s00477-020-01776-2.

Becker, W. (2020). Meta functions for benchmarking in sensitivity analysis. Reliability Engineering & System Safety, 204, 107189. https://doi.org/10.1016/j.ress.2020.107189.

Bouffard, D., Kiefer, I., Wüest, A., Wunderle, S., & Odermatt, D., (2018). Are surface temperature and chlorophyll in a large deep lake related? An analysis based on satellite observations in synergy with hydrodynamic modelling and in-situ data. Remote Sens. Environ. 209, 510–523. https://doi.org/10.1016/j.rse.2018.02.056 https://doi.org/.

Breiman, L. (2001). Random forests. Machine learning, 45, 5-32.

Brokamp, C., Jandarov, R., Hossain, M., & Ryan, P. (2018). Predicting daily urban fine particulate matter concentrations using a Random Forest model. Environ. Sci. Technol. 52, 4173–4179. https://doi.org/10.1021/acs.est.7b05381.

Campolongo, F., Cariboni, J., & Saltelli, A. (2007). An effective screening design for sensitivity analysis of large models. Environ. Modelling & Software, Modelling, Comput. Assisted Simul. Map. Dangerous Phenomena for Hazard Assess. 22, 1509–1518. https://doi.org/10.1016/j.envsoft.2006.10.004.

Chen, T., & Guestrin, C. (2016). Xgboost: A scalable tree boosting system, in: Proceedings of the 22nd Acm Sigkdd International Conference on Knowledge Discovery and Data Mining, ACM, 2016, pp. 785–794. https://doi.org/10.1145/2939672.2939785.

Chen, K., Chen, H., Zhou, C., Huang, Y., Qi, X., Shen, R., & Ren, H. (2020). Comparative analysis of surface water quality prediction performance and identification of key water parameters using different machine learning models based on big data. Water Res. 171, 115454. https://doi.org/10.1016/j.watres.2019.115454.

COSIA (2012). Technical Guide for Fluid Fine Tailings Management. Canadian Oil Sands Innovation Alliance, Edmonton, AB. August 2012. Report, 1-131. [Available at http://www.cosia.ca /initiatives /project-research, last accessed 27 September 2023.]

Cossey, H. L., Batycky, A. E., Kaminsky, H., & Ulrich, A. C. (2021). Geochemical stability of oil sands tailings in mine closure landforms. Minerals, 11(8), 830. https://doi.org/10.3390/ min11080830.

Coyle, D., & Weller, A. (2020). "Explaining" machine learning reveals policy challenges. science, 368(6498), 1433-1434. https://doi.org/10.1126/science.aba9647.

Cupe-Flores, B., Mendes, M., Panigrahi, B., & Liber, K. (2022). Delineating effluent exposure and cumulative ecotoxicological risk of metals downstream of a Saskatchewan uranium mill using autonomous sensors. Environmental Toxicology and Chemistry 41, 1765-1777. http://dx.doi.org/10.1002/etc.5341.

De la Fuente, L. A., Gupta, H. V., & Condon, L. E. (2023). Toward a Multi-Representational Approach to Prediction and Understanding, in Support of Discovery in Hydrology. Water Resources Research, 59(1), e2021WR031548.

Do, N. C., & Razavi, S., (2020). Correlation effects? A major but often neglected component in sensitivity and uncertainty analysis. Water Resources Research, 56, e2019WR025436. https://doi.org/10.1029/2019WR025436.

Dompierre, K. A., Lindsay, M. B. J., Cruz-Hernández, P., & Halferdahl, G. M. (2016). Initial geochemical characteristics of fluid fine tailings in an oil sands end pit lake, Sci. Total Environ., Science of the Total Environment 556, 196-206. https://doi.org/10.1016/ j.scitotenv.2016.03.002.

Dompierre, K.A., & Barbour, S.L. (2016). Characterization of physical mass transport through oil sands fluid fine tailings in an end pit lake: A multi-tracer study, J. Contam. Hydrol., 189(1), 12–26. https://doi.org/10.1016/j.jconhyd.2016.03.006.

Fatichi, S., Vivoni, E. R., Ogden, F. L., Ivanov, V. Y., Mirus, B., Gochis, D., Downer, C. W., Camporese, M., Davison, J. H., Ebel, B., Jones, N., Kim, J., Mascaro, G., Niswonger, R., Restrepo, P., Rigon, R., Shen, C., Sulis, M., & Tarboton, D. (2016). An overview of current applications, challenges, and future trends in distributed process-based models in hydrology. Journal of Hydrology, 537, 45–60. https://doi.org/10.1016/J.JHYDROL.2016.03.026.

Fel, T., Cadene, R., Chalvidal, M., Cord, M., Vigouroux, D., & Serre, T. (2021) Look at the variance! Efficient black-box explanations with Sobol-based sensitivity analysis. In Beygelzimer, A., Dauphin, Y., Liang, P., and Vaughan, J. W. (eds.), Advances in Neural Information Processing Systems, 2021. URL https://openreview.net/forum?id=hA-PHQGOjqQ.

Freund, Y., & Schapire, R. E. (1997). A desicion-theoretic generalization of on-line learning and an application to boosting J. Comput. Syst. Sci., 55 (1997), pp. 23-37.

Friedman, J. H. (1991). Multivariate adaptive regression splines. The annals of statistics, 19(1), 1-67. https://doi.org/10.1214/aos/1176347963.

Friedman J. H. (2001). Greedy function approximation: a gradient boosting machine, Ann. Statist. (2001) 1189–1232. https://www.jstor.org/stable/2699986.

649 Frye, C., Rowat, C., & Feige, I. (2020). Asymmetric shapley values: incorporating causal knowledge into model-
650 agnostic explainability. Advances in Neural Information Processing Systems, 33, 1229-1239.

651 Garosi, Y., Sheklabadi, M., Conoscenti, C., Pourghasemi, H. R., & Van Oost, K. (2019). Assessing the performance
652 of GIS-based machine learning models with different accuracy measures for determining susceptibility
653 to gully erosion. Science of the Total Environment, 664, 1117-1132.
654 https://doi.org/10.1016/j.scitotenv.2019.02.093.

655 Gosselin, P., Hrudey, S. E., Naeth, M. A., Plourde, A., Therrien, R., Kraak, G. V. D., & Xu, Z. (2010). Environmental
656 and Health Impacts of Canada's Oils Sands Industry, R. Soc. of Canada, Ottawa, Canada.

657 Haghnegahdar, A., & Razavi, S. (2017). Insights into sensitivity analysis of Earth and environmental systems
658 models: On the impact of parameter perturbation scale. Environmental Modelling & Software, 95, 115-
659 131. http://dx.doi.org/10.1016/j.envsoft.2017.03.031.

660 Harrison, J. W., Beecraft, L., & Smith, R. E. H. (2018). Implications of irradiance exposure and non-
661 photochemical quenching for multi-wavelength (bbe FluoroProbe) fluorometry. J. Photochem.
662 Photobiol. B Biol. 189, 36–48. https://doi.org/10.1016/j.jphotobiol. 2018.09.013.

663 Hipsey, M. R., Hamilton, D. P., Hanson, P. C., Carey, C. C., Coletti, J. Z., Read, J. S., Ibelings, B. W., Valesini, F. J.,
664 & Brookes, J. D. (2015). Predicting the resilience and recovery of aquatic systems: A framework for model
665 evolution within environmental observatories. Water Resources Research, 51, 7023–7043.
666 https://doi.org/10.1002/2015WR017175.

667 Homma, T., & Saltelli, A. (1996). Importance measures in global sensitivity analysis of nonlinear models.
668 Reliability Engineering & System Safety, 52(1):1–17. https://doi.org/10.1016/0951-8320(96)00002-6.

669 Janzing, D., Minorics, L., & Blöbaum, P. (2020). Feature relevance quantification in explainable AI: A causal
670 problem. In International Conference on artificial intelligence and statistics, PMLR, 2020, pp. 2907-2916.

671 Jeihouni, M., Toomanian, A., & Mansourian, A. (2020). Decision tree-based data mining and rule induction for
672 identifying high quality groundwater zones to water supply management: a novel hybrid use of data
673 mining and GIS. Water Resour. Manag. 34, 139–154. https://doi.org/10.1007/s11269-019-02447-w.

674 Kambhatla, N., & Leen, T. K. (1997). Dimension reduction by local principal component analysis. Neural
675 Comput. 9, 1493–1516. https://doi.org/10.1162/neco.1997.9.7.1493.

676 Ke, G., Meng, Q., Finley, T., Wang, T., Chen, W., Ma, W., Ye, Q., & Liu, T. Y. (2017). LightGBM: A highly efficient
677 gradient boosting decision tree, in: Advances in Neural Information Processing Systems, pp. 3146–3154.

678 Khullar, S., & Singh, N. (2021). Water quality assessment of a river using deep learning Bi-LSTM methodology:
679 forecasting and validation. Environmental Science and Pollution Research, 29(9), 12875-12889.
680 https://doi.org/10.1007/s11356-021-13875-w.

681 Kim, H., & Kim, B. (2020). Analysis of major rainfall factors affecting inundation based on observed rainfall and
682 Random Forest. Korean Soc. Hazard Mitig. 20, 301–310.
683 https://doi.org/10.9798/KOSHAM.2020.20.6.301.

684 Kleijnen, J. P. C. (1995). Sensitivity analysis and optimization of system dynamics models: regression analysis
685 and statistical design of experiments. Syst. Dynam. Rev. 11, 275–288.
686 https://doi.org/10.1002/sdr.4260110403.

687 Konapala, G., & Mishra, A. (2020). Quantifying climate and catchment control on hydrological drought in the
688 continental United States. Water Resources Research, 56 (1). https://doi.org/10.1029/2018WR024620.

689 Kucherenko, S., & Iooss, B. (2016). Derivative-based global sensitivity measures. In Handbook of Uncertainty
690 Quantification, pp. 1–24. Springer International Publishing, Cham. https://doi.org/10.1007/978-3-319-
691 11259-6 36-1.

Kucherenko, S., & Song, S. (2016). Derivative-based global sensitivity measures and their link with Sobol' sensitivity indices. Monte Carlo and Quasi-Monte Carlo Methods, pp. 455–469. https://doi.org/10.1007/978-3-319-33507-0 23.

Kuhnt, S. & Kalka, A. (2022). Global sensitivity analysis for the interpretation of machine learning algorithms, pp. 155–169. Springer International Publishing, Cham, 2022. https://doi.org/10.1007/978-3-031-07155-3 6.

Kumar, I. E., Venkatasubramanian, S., Scheidegger, C., & Friedler, S. (2020). Problems with Shapley-value-based explanations as feature importance measures. In International Conference on Machine Learning (pp. 5491-5500). Proceedings of Machine Learning Research (PMLR). https://proceedings.mlr.press/v119/kumar20e/kumar20e.pdf.

Lakkaraju, H., Kamar, E. Caruana, R., & Leskovec. J. (2019). Faithful and customizable explanations of black box models. In Proceedings of the 2019 AAAI/ACM Conference on AI, Ethics, and Society. 131–138.

Lakkaraju, H. & Bastani, O. (2020). How do I fool you? Manipulating user trust via misleading black box explanations. In Proceedings of the AAAI/ACM Conference on AI, Ethics, and Society (pp. 79-85).

Lamboni, M., Iooss, B., Popelin, A.L., & Gamboa, F. (2013). Derivative-based global sensitivity measures: general links with Sobol' indices and numerical tests. Math. Comput. Simulat. 87, 45–54. https://doi.org/10.1016/j.matcom.2013.02.002.

Liakos, K. G., Busato, P., Moshou, D., Pearson, S., & Bochtis, D. (2018). Machine learning in agriculture: A review. Sensors, 18(8), 2674. https://doi.org/10.3390/s18082674.

Libelium (2020). Technical Guide-Smart Water Extreme, Document version: v7.3- 02/2020. https://www.scribd.com/document/375986458/Waspmote-Technical-Guide.

Lipton, Z. C. (2017). The Mythos of Model Interpretability: In Machine Learning, the Concept of Interpretability Is Both Important and Slippery. Queue, 16, 31–57. https://arxiv.org/pdf/1606.03490.pdf.

Liu, H., Clark, M. P., Gharari, S., Sheikholeslami, R., Freer, J., Knoben, W. J. M., Marsh, C. B., & Papalexiou, S. M. (2024). An improved copula-based framework for efficient global sensitivity analysis. Water Resources Research, 60, e2022WR033808. https://doi.org/10.1029/2022WR033808.

Liu, X., & Georgakakos, A. P. (2021). Chlorophyll a estimation in lakes using multi-parameter sonde data, Water Research, Volume 205, 117661, ISSN 0043-1354, https://doi.org/10.1016/j.watres.2021.117661.

Lundberg, S. M., & Lee, S. I. (2017). A unified approach to interpreting model predictions. Advances in neural information processing systems, 30. https://doi.org/10.48550/arXiv.1705.07874.

Lundberg, S. M., Erion, G., Chen, H., DeGrave, A., Prutkin, J. M., Nair, B., Katz, R., Himmelfarb, J., Bansal, N., & Lee, S. I. (2020). From local explanations to global understanding with explainable AI for trees, Nature Machine Intelligence, Vol 56-67. https://doi.org/ 10.1038/s42256-019-0138-9.

Maier, H. R., Galelli, S., Razavi, S., Castelletti, A., Rizzoli, A., Athanasiadis, I. N., Sanchez-Marre, M., Acutis, M., Wu, W., & Humphrey, G. B. (2023). Exploding the myths: An introduction to artificial neural networks for prediction and forecasting. Environmental modelling & software, 105776. https://doi.org/10.1016/j.envsoft.2023.105776.

Mase, M., Owen, A. B., & Seiler, B. (2019). Explaining black box decisions by shapley cohort refinement. arXiv preprint arXiv:1911.00467.

McNeill, J. (2017). Alberta Government continues its mismanagement of fluid tailings with approval of CNRL's tailings plan: Pembina Institute reacts to Alberta Energy Regulator's decision. https://www.pembina.org/media-release.

Molnar, C., König, G., Herbinger, J., Freiesleben, T., Dandl, S., Scholbeck, C. A., Casalicchio, G., Grosse-Wentrup, M. & Bischl, B. (2020). Pitfalls to avoid when interpreting machine learning models.

Molnar, C. (2022) Interpretable Machine Learning. 2nd edition, 2022. URL https://christophm.github.io/interpretable-ml-book.

Morris, M. D. (1991). Factorial sampling plans for preliminary computational experiments. Technometrics 33, 161–174. https://doi.org/10.1080/00401706.1991.10484804.

Mosavi, A., Hosseini, S. F., Choubin, B., Goodarzi, M., Dineva, A. A., & Sardooi, R. E. (2021). Ensemble boosting and bagging based machine learning models for groundwater potential prediction. Water Resources Management, 35, 23-37. https://doi.org/10.1007/s11269-020-02704-3.

Najah, A., El-Shafie, A., Karim, O.A., & El-Shafie, A.H. (2014). Performance of ANFIS versus MLP-NN dissolved oxygen prediction models in water quality monitoring. Environ. Sci. Pollut. Res. 2014, 21, 1658–1670. https://doi.org/10.1007/s11356-013-2048-4.

Nossent, J., Elsen, P., & Sobol', B.W. (2011). Sensitivity analysis of a complex environmental model. Environmental Modelling & Software, 26(12):1515–1525, 2011. https://doi.org/10.1016/j.envsoft.2011.08.010.

Ojha, V., Timmis, J., & Nicosia, G. (2022). Assessing ranking and effectiveness of evolutionary algorithm hyperparameters using global sensitivity analysis methodologies. Swarm and Evolutionary Computation, 74,101130. https://doi.org/10.1016/j.swevo.2022.101130.

Owen, A. (1994). Lattice Sampling Revisited: Monte Carlo Variance of Means Over Randomized Orthogonal Arrays. Ann. Statist. 22, 930–945. https://doi.org/10.1214/aos/1176325504.

Owen, A. (2014). Sobol' indices and Shapley value. SIAM/ASA Journal on Uncertainty Quantification, 2:245–251, 01 2014. https://doi.org/10.1137/130936233.

Paleari, L., Movedi, E., Zoli, M., Burato, A., Cecconi, I., Errahouly, J., Pecollo, E., Sorvillo, C., & Confalonieri, R. (2021). Sensitivity analysis using Morris: Just screening or an effective ranking method? Ecological Modelling, 455: 109648, 2021. https://doi.org/10.1016/j.ecolmodel. 2021.109648.

Palani, S., Liong, S.Y., & Tkalich, P. (2008). An ANN application for water quality forecasting. Mar. Pollut. Bull. 56, 1586–1597. https://doi.org/10.1016/j.marpolbul.2008.05.021.

Pedregosa, F., Varoquaux, G., Gramfort, A., Michel, V., Thirion, B., Grisel, O., Blondel, M., Prettenhofer, P., Weiss, R., Dubourg, V., Vanderplas, J., Passos, A., & Duchesnay, É. (2011). Scikit-learn: Machine learning in Python. the Journal of machine Learning research, 12, 2825-2830.

Peixoto Mendes, M., Cupe-Flores, B., Panigrahi, B., & Liber, K. (2023). Application of autonomous sensor technology to estimate selenium exposure and a site-specific selenium threshold in a Canadian boreal lake. Integrated Environmental Assessment and Management 19, 395-411. http://dx.doi.org/10.1002/ieam.4644.

Pena, M., Katsev, S., Oguz, T., & Gilbert, D. (2010). Modeling dissolved oxygen dynamics and hypoxia. Biogeosciences, 7 (3), 933−957. https://doi.org/10.5194/bg-7-933-2010.

Puy, A., Becker, W., Lo Piano, S., & Saltelli, A. A. (2021). comprehensive comparison of total-order estimators for global sensitivity analysis. International Journal for Uncertainty Quantification. https://doi.org/10.1615/int.j.uncertaintyquantification.2021038133.

Puy, A., Beneventano, P., Levin, S. A., Lo Piano, S., Portaluri, T., & Saltelli, A. (2022). Models with higher effective dimensions tend to produce more uncertain estimates. Science Advances, 8(42), https://doi.org/10.1126/sciadv.abn945.

Rahmati, O., Tahmasebipour, N., Haghizadeh, A., Pourghasemi, H. R., & Feizizadeh, B. (2017). Evaluation of different machine learning models for predicting and mapping the susceptibility of gully erosion. Geomorphology, 298, 118-137. https://doi.org/ 10.1016/j.geomorph.2017.09.006.

779 Rakovec, O., Hill, M. C., Clark, M. P., Weerts, A. H., Teuling, A. J., & Uijlenhoet, R. (2014). Distributed Evaluation
780 of Local Sensitivity Analysis (DELSA), with application to hydrologic models: distributed evaluation of
781 local sensitivity analysis. Water Resour. Res. 50, 409–426. https://doi.org/10.1002/2013WR014063.

782 Razavi, S., & Gupta, H.V. (2015). What do we mean by sensitivity analysis? The need for comprehensive
783 characterization of "global" sensitivity in Earth and Environmental systems models: a Critical Look at
784 Sensitivity Analysis. Water Resour. Res. 51, 3070–3092. https://doi.org/10.1002/2014WR016527.

785 Razavi, S., & Gupta, H. V. (2016a). A new framework for comprehensive, robust, and efficient global sensitivity
786 analysis: 1. Theory. Water Resour. Res. 52, 423–439. https://doi.org/10.1002/2015WR017558.

787 Razavi, S., & Gupta, H. V. (2016b). A new framework for comprehensive, robust, and efficient global sensitivity
788 analysis: 2. Application. Water Resour. Res. 52, 440–455. https://doi.org/10.1002/2015WR017559.

789 Razavi, S. (2021). Deep learning, explained: Fundamentals, explainability, and bridgeability to process-based
790 modelling. Environmental Modelling & Software, 144:105159, 2021. doi:
791 https://doi.org/10.1016/j.envsoft.2021.105159.

792 Razavi, S., Jakeman, A., Saltelli, A., Prieur, C., Iooss, B., Borgonovo, E., Plischke, E., Piano, L. S., Iwanaga, T., Becker,
793 W., Tarantola, S., Guillaume, J. H., Jakeman, J., Gupta, H., Melillo, N., Rabitti, G., Chabridon, V., Duan, Q.,
794 Sun, X., Smith, S., Sheikholeslami, R., Hosseini, N., Asadzadeh, M., Puy, A., Kucherenko, S., & Maier, H. R.
795 (2021). The Future of Sensitivity Analysis: An essential discipline for systems modeling and policy support,
796 Environmental Modelling and Software 137 (2021) 104954,
797 https://doi.org/10.1016/j.envsoft.2020.104954.

798 Razavi, S., Hannah, D. M., Elshorbagy, A., Kumar, S., Marshall, L., Solomatine, D. P., Dezfuli, A., Sadegh, M., &
799 Famiglietti, J. (2022). Coevolution of machine learning and process-based modelling to revolutionize
800 Earth and environmental sciences: A perspective. Hydrological Processes, 36(6).
801 https://doi.org/10.1002/hyp.14596.

802 Read, J. S., Jia, X., Willard, J., Appling, A. P., Zwart, J. A., Oliver, S. K., Karpatne, A., Hansen, G. J. A., Hanson, P.
803 C., Watkins, W., Steinbach, M., & Kumar, V. (2019). Process-guided deep learning predictions of lake
804 water temperature. Water Resources Research, 55, https://doi.org/10.1029/2019WR024922.

805 Ribeiro, M. T., Singh, S., & Guestrin, C. (2016). Why should i trust you? Explaining the predictions of any
806 classifier. In Proceedings of the 22nd ACM SIGKDD international conference on knowledge discovery and
807 data mining (pp. 1135-1144).

808 Risacher, F. F., Morris, P. K., Arriaga, D., Goad, C., Nelson, T. C., Slater, G. F., & Warren, L. A. (2018). The interplay
809 of methane and ammonia as key oxygen consuming constituents in early stage development of Base
810 Mine Lake, the first demonstration oil sands pit lake, Applied Geochemistry, Volume 93, 2018, Pages 49-
811 59, ISSN 0883-2927, https://doi.org/10.1016/j.apgeochem.2018.03.013.

812 Roscher, R., Bohn, B., Duarte, A., & Garcke, J. (2020). Explainable Machine Learning for Scientific Insights and
813 Discoveries 10.1109/ACCESS.2020.2976199.

814 Roskosch, A., Hette, N., Hupfer, M., & Lewandowski, J. (2012). Alteration of Chironomus plumosus ventilation
815 activity and bioirrigation-mediated benthic fluxes by changes in temper ature, oxygen concentration,
816 and seasonal variations. Fresh water Science 31:269–281.

817 Rudin, S. (2019). Stop Explaining Black Box Machine Learning Models for High Stakes Decisions and Use
818 Interpretable Models Instead. Nat. Mach. Intell, 1, 206–215.

819 Rudin, C., Chen, C., Chen, Z., Huang, H., Semenova, L., & Zhong, C. (2022). Interpretable machine learning:
820 Fundamental principles and 10 grand challenges. Statistics Surveys, 16:1 – 85, 2022.
821 https://doi.org/10.1214/21-SS133.

822 Saltelli, A., Jakeman, A., Razavi, S., & Wu, Q. (2021). Sensitivity analysis: A discipline coming of age.
823 Environmental Modelling & Software, 146, 105226. https://doi.org/10.1016/ j.envsoft.2021.105226.

Sameen, M. I., Pradhan, B., & Lee, S. (2019). Self-learning random forests model for mapping groundwater yield in data-scarce areas. Natural Resources Research, 28, 757-775. https://doi.org/10.1007/s11053-018-9416-1.

Samek, W., Montavon, G., Vedaldi, A., Hansen, L. K. & Müller, K. R. (2019). Explainable AI: Interpreting, Explaining and Visualizing Deep Learning; Lecture Notes in Artificial Intelligence, Lect.Notes ComputerState-of-the-Art Surveys; Springer: Berlin/Heidelberg, Germany, ISBN 978-3-030-28953-9.

Sánchez, E., Colmenarejo, M. F., Vicente, J., Rubio, A., García, M. G., Travieso, L., & Borja, R. (2006). Use of the water quality index and dissolved oxygen deficit as simple indicators of watersheds pollution. Ecol. Indic. 2007, 7 (2), 315−328. https://doi.org/10.1016/ j.ecolind.2006.02.005.

Sasar M., Johnston C. T., & Santagata M. (2022). Characterization and Dynamics of Residual Organics in Oil Sands Fluid Fine Tailings. Energy Fuels 2022, 36, 6881−689. https://doi.org/10.1021/acs.energyfuels.2c01315.

Savoy, P., & Harvey, J. W. (2023). Predicting daily river chlorophyll concentrations at a continental scale. Water Resources Research, 59, e2022WR034215. https://doi.org/10.1029/2022WR034215.

Scholbeck, C. A., Moosbauer, J., Casalicchio, G., Gupta, H., Bischl, B., & Heumann, C. (2023). Position Paper: Bridging the Gap Between Machine Learning and Sensitivity Analysis. arXiv preprint arXiv:2312.13234.

Shammas, N., Wang, L., & Wu, Z. (2009). Waste Stabilization Ponds and WSPs, in Volume 8: Biological Treatment Processes, Handbook of Environmental Engineering, Humana Press, Totowa, New Jersey, pp. 315–370.

Sheikholeslami, R., Gharari, S., Papalexiou, S. M., & Clark, M. P. (2021). VISCOUS: A variance-based sensitivity analysis using copulas for efficient identification of dominant hydrological processes. Water Resources Research, 57, e2020WR028435. https://doi. org/10.1029/2020WR028435.

Sheikholeslami, R., & Razavi, S. (2020). A fresh look at variography: measuring dependence and possible sensitivities across geophysical systems from any given data. Geophysical Research Letters, 47(20). https://doi.org/10.1029/2020GL089829.

Sheikholeslami, R., Razavi, S., Gupta, H.V., Becker, W., & Haghnegahdar, A. (2019). Global sensitivity analysis for high-dimensional problems: how to objectively group factors and measure robustness and convergence while reducing computational cost. Environ. Model. Software 111, 282–299. https://doi.org/10.1016/j.envsoft.2018.09.002.

Sheikholeslami, R., Yassin, F., Lindenschmidt, K. E., & Razavi, S. (2017). Improved understanding of river ice processes using global sensitivity analysis approaches. Journal of Hydrologic Engineering, 22(11). https://doi.org/10.1061/(ASCE)HE.1943-5584.0001574.

Shin, M.-J., Guillaume, J. H., Croke, B. F., & Jakeman, A. J. (2013) Addressing ten questions about conceptual rainfall– runoff models with global sensitivity analyses in R. Journal of Hydrology, 503:135–152, 2013. https://doi.org/10.1016/j.jhydrol.2013.08.047.

Sinshaw, T.A., Surbeck, C.Q., Yasarer, H., & Najjar Y. (2019). Artificialnneural network for prediction of total nitrogen and phosphorus in US lakes. J Environ Eng 145(6):04019032. https://doi.org/10.1061/(ASCE)EE.1943-7870.0001528.

Slack, D., Hilgard, A., Singh, S., & Lakkaraju, H. (2021). Reliable post hoc explanations: Modeling uncertainty in explainability. Advances in neural information processing systems, 34, 9391-9404.

Slack, D., Krishna, S., Lakkaraju, H., & Singh, S. (2023). Explaining machine learning models with interactive natural language conversations using TalkToModel. Nature Machine Intelligence, 5(8), 873-883. https://doi.org/10.1038/s42256-023-00692-8.

Sobol', I. M. (1993). Sensitivity analysis for non-linear mathematical models. Mathematical Modelling and Computational Experiment, Translated from Russian: I.

M. Sobol', Sensitivity estimates for nonlinear mathematical models. Matematicheskoe Modelirovanie 2, 407–414 (1990) 112–118 1.

Sobol, I. M. (2001). Global sensitivity indices for nonlinear mathematical models and their Monte Carlo estimates. MATH COMPUT SIMULAT,55(1–3),271-280, https://doi.org/10.1016/S0378-4754(00)00270-6.

Sobol', I. M., & Kucherenko, S. (2009). Derivative based global sensitivity measures and their link with global sensitivity indices. Math. Comput. Simulat. 79, 3009–3017. https://doi.org/10.1016/j.matcom.2009.01.023.

Song, X., Zhang, J., Zhan, C., Xuan, Y., Ye, M., & Xu, C. (2015). Global sensitivity analysis in hydrological modeling: Review of concepts, methods, theoretical framework, and applications. Journal of Hydrology, 523:739–757, 2015. https://doi.org/10.1016/j.jhydrol.2015.02.013.

Song, E., Nelson, B. L., & Staum, J. (2016). Shapley effects for global sensitivity analysis: Theory and computation. SIAM/ASA Journal on Uncertainty Quantification, 4(1), 1060-1083. https://doi.org/10.1137/15M1048070.

Stein, B. V., Raponi, E., Sadeghi, Z., Bouman, N., Van Ham, R. C. H. J., & Back, T. (2022). A comparison of global sensitivity analysis methods for explainable AI with an application in genomic prediction. IEEE Access, 10:103364–103381.

Strobl, C., Boulesteix, A. L., Kneib, T., Augustin, T., & Zeileis, A. (2008). Conditional variable importance for random forests. BMC bioinformatics, 9, 1-11. https://doi:10.1186/1471-2105-9-307.

Strumbelj, E., & Kononenko, I. (2014). Explaining prediction models and individual predictions with feature contributions. Knowledge and Information Systems, 41(3): 647–665, Dec 2014.

Stumm, W., & Morgan, J. J. (2012). Aquatic chemistry: chemical equilibria and rates in natural waters. John Wiley & Sons.

Tonkin, M. J., & Doherty, J. (2005). A hybrid regularized inversion methodology for highly parameterized environmental models: hybrid regularization methodology. Water Resour. Res. 41 https://doi.org/10.1029/2005WR003995.

Torres-Barrán, A., Alonso, Á., & Dorronsoro, J. R. (2019). Regression tree ensembles for wind energy and solar radiation prediction. Neurocomputing, 326, 151-160. http://dx.doi.org/10.1016/j.neucom.2017.05.104.

Tunkiel, A. T., Sui, D., & Wiktorski, T. (2020). Data-driven sensitivity analysis of complex machine learning models: A case study of directional drilling. Journal of Petroleum Science and Engineering, 195:107630, 2020. https://doi.org/10.1016/j.petrol.2020.107630.

Veeresh, M., Veeresh, A. V, Huddar B. D., & Hosetti, B. B. (2010). Dynamics of industrial waste stabilization pond treatment processes, Environ. Monit. Assess., 169, 55–65. https://doi.org/10.1007/s10661-009-1150-z.

Wallace, J., Champagne, P. & Hall, G. (2016). Time series relationships between chlorophyll-a, dissolved oxygen, and pH in three facultative wastewater stabilization ponds, Environ. Sci.: Water Res. Technol., 2016, 2, 1032. https://doi.org/10.1039/C6EW00202A.

Wang, F., Wang, Y., Zhang, K., Hu, M., Weng, Q., & Zhang, H. (2021). Spatial heterogeneity modeling of water quality based on random forest regression and model interpretation. Environmental Research, 202, 111660. https://doi.org/10.1016/j.envres.2021.111660.

Wang, H., Jasim, A., & Chen, X. (2018). Energy harvesting technologies in roadway and bridge for different applications–A comprehensive review. Appl. Energy 212, 1083–1094. https://doi.org/10.1016/j.apenergy.2017.12.125.

Wang, P., Lu, B., Zhang, H., Zhang, W., Su, Y., & Ji, Y. (2014). Water demand prediction model based on random forests model and its application. Water Resour. Prot. 30, 34–37.

Wetzel, R. G. (2001). Limnology: Lake and river ecosystems. 3rd ed., Academic press, San Diego. 1006p.

Wu, Y., & Chen, J. (2013). Investigating the effects of point source and nonpoint source pollution on the water quality of the East River (Dongjiang) in South China. Ecol Indic 32:294–304. https://doi.org/10.1016/j.ecolind.2013.04.002.

Wu, Y., & Liu, S. (2012). Modeling of land use and reservoir effects on nonpoint source pollution in a highly agricultural basin. J Environ Monit 14(9):2350–2361. https://doi.org/10.1039/C2EM30278K.

Xie, M., Wang, N., Gaillard, J. F., & Packman, A. I. (2018). Interplay between flow and bioturbation enhances metal efflux from low-permeability sediments. J. Hazard Mater. 341, 304–312. https://doi.org/10.1016/j.jhazmat.2017.08.002.

Yim, I., Shin, J., Lee, H., Park, S., Nam, G., Kang, T., Cho, K.H., & Cha, Y. (2020). Deep learning-based retrieval of cyanobacteria pigment in inland water for in-situ and airborne hyperspectral data. Ecological Indicators, 110, 105879. https://doi.org/10.1016/ j.ecolind.2019.105879.

Yamamoto, R., Harada, M., Hiramatsu, K., & Tabata, T. (2021). Three-layered Feedforward artificial neural network with dropout for short-term prediction of class-differentiated Chl-a based on weekly water-quality observations in a eutrophic agricultural reservoir. Paddy and Water Environment, 1-18. https://doi.org/10.1007/s10333-021-00874-3.

Zhang, W., Han, S., Zhang, D., Jin, X., Cao, E., Shan, B., & Wei, D. (2022). Preliminary Study on the Dissolved Oxygen Recovery Process in Freshwater Ecosystems under the Coupling Effect of Oxygen-Consuming Pollutants and Temperature. ACS ES&T Water 2, 1639-1646. http://dx.doi.org/10.1021/acsestwater.2c00150

Zhang, Y., Yao, X., Wu, Q., Huang, Y., Zhou, Z., Yang, J., & Liu, X. (2021). Turbidity prediction of lake-type raw water using random forest model based on meteorological data: A case study of Tai lake, China. Journal of Environmental Management, 290, 112657. https://doi.org/10.1016/j.jenvman.2021.112657.

Zhou, C., & Zhang, J. (2023). Simultaneous measurement of chemical oxygen demand and turbidity in water based on broad optical spectra using backpropagation neural network. Chemometrics and Intelligent Laboratory Systems, 237, 104830. https://doi.org/10.1016/j.chemolab.2023.104830.

Zou, X. Y., Lin, Y. L., Xu, B., Guo, Z. B., Xia, S. J., Zhang, T. Y., & Gao, N. Y. (2019). A novel event detection model for water distribution systems based on data-driven estimation and support vector machine classification. Water Resour. Manag. 33 (13), 4569–4581. https://doi.org/10.1007/s11269-019-02317-5.